environmental microbiology

Environmental Microbiology (2019) **00**(00), 00–00 doi:10.1111/1462-2920.14567

The Y233 gatekeeper of DmpR modulates effector-responsive transcriptional control of σ^{54}-RNA polymerase

Henrik Seibt,[1] Uwe H. Sauer[2] and Victoria Shingler[1*]

[1]*Department of Molecular Biology, Umeå University, SE-901 87, Umeå, Sweden.*

[2]*Deparment of Chemistry, Umeå University, SE-901 87, Umeå, Sweden.*

Summary

DmpR is the obligate transcriptional activator of genes involved in (methyl)phenol catabolism by *Pseudomonas putida.* DmpR belongs to the AAA$^+$ class of mechano-transcriptional regulators that employ ATP-hydrolysis to engage and remodel σ^{54}-RNA polymerase to allow transcriptional initiation. Previous work has established that binding of phenolic effectors by DmpR is a prerequisite to relieve interdomain repression and allow ATP-binding to trigger transition to its active multimeric conformation, and further that a structured interdomain linker between the effector- and ATP-binding domains is involved in coupling these processes. Here, we present evidence from ATPase and *in vivo* and *in vitro* transcription assays that a tyrosine residue of the interdomain linker (Y233) serves as a gatekeeper to constrain ATP-hydrolysis and aromatic effector-responsive transcriptional activation by DmpR. An alanine substitution of Y233A results in both increased ATPase activity and enhanced sensitivity to aromatic effectors. We propose a model in which effector-binding relocates Y233 to synchronize signal-reception with multimerisation to provide physiologically appropriate sensitivity of the transcriptional response. Given that Y233 counterparts are present in many ligand-responsive mechano-transcriptional regulators, the model is likely to be pertinent for numerous members of this family and has implications for development of enhanced sensitivity of biosensor used to detect pollutants.

Received 8 December, 2018; revised 13 February, 2019; accepted 14 February, 2019. *For correspondence. E-mail vicky.shingler@umu.se; Tel. +46 90 785 2534; Fax +46 90 772 630.

Introduction

Members of the XylR/DmpR subfamily of σ^{54}-dependent mechano-transcriptional activators play pivotal roles in controlling bacterial degradation of aromatic compound (Shingler, 2003; Tropel and van der Meer, 2004). DmpR is the master regulator required for production of a suite of nine enzymes of the (methyl)phenol catabolic pathway of *Pseudomonas putida* CF600 (Shingler *et al*., 1993). This pathway confers the ability to grow at the expense of a variety of methylated phenolic compounds as sole carbon and energy sources (reviewed in Shingler, 2004). This subfamily contains many well characterized members, including the DmpR-like MopR and PoxR proteins, which are all direct sensors of phenolic compounds (Schirmer *et al*., 1997; Patil *et al*., 2016; Ray *et al*., 2016). This subfamily has attracted particular interest because of their ability to directly bind aromatic pollutants and their consequent use in environmental biosensors applications (e.g. Garmendia *et al*., 2001; van der Meer and Belkin, 2010; Xue *et al*., 2014; Shingler, 2017).

Initiation of transcription by σ^{54}-RNA polymerase strictly requires activation by ATP-driven mechano-transcriptional regulators. These mechano-activators use ATP-hydrolysis to remodel σ^{54}-RNA polymerase locked in an inactive closed promoter complex to allow formation of the open promoter complex and, thus, transcriptional initiation (Zhang *et al*., 2016). The activation process is generally mediated by the activator bound to DNA sequences located approximately 100–200 base pairs upstream from the σ^{54}-promoter they control, thus lending the family the name bacterial enhancer binding proteins (bEBPs).

DmpR, as is typical of most bEBPs, is comprised of an N-terminal signal reception A-domain, an interdomain B-linker that tethers the A-domain to a central AAA$^+$ C-domain followed by a DNA binding D-domain at its C-terminus. The AAA$^+$ (ATPase associated with various cellular activities) scaffold of the C-domain encompasses the walker A (P-loop) and walker B motifs required for ATP-binding and hydrolysis. This domain also encompasses bEBP-specific regions that are the hallmark of the family, namely the mobile GAFTGA/loop1 and loop 2, which are employed in productive coupling and energy transfer from bEBP

nucleotide hydrolysis to remodelling of σ^{54}-RNAP (Rappas *et al*., 2007; Bose *et al*., 2008).

As the name implies, the signal reception A-domain of bEBPs control transition to the active multmeric form. Most bEBPs exist as inactive dimers with their activity controlled in response to environmental signals leading to a transition into active oligomers – usually ring-shaped hexamers. In addition to ligand-binding, A-domain mediated control mechanisms include phosphorylation cascades and signal-responsive protein–protein interactions. Signalling via the A-domain results in conformational changes so that the A-domain in some classes of bEBP stabilizes the active form, or in others, relieves interdomain repression to allow subsequent multimerisation to the active configuration (reviewed in Shingler, 2011; Bush and Dixon, 2012). DmpR belongs to the latter class, with its A-domain mediating repression of the catalytic and self-association properties of the central C-domain when effectors are absent (Ng *et al*., 1996; O'Neill *et al*., 1998; 1999; Wikstrom *et al*., 2001).

Binding of phenolic effectors stimulates the intrinsic ATPase activity of DmpR – a process that is mimicked by removal of the A-domain, which results in a derivative that has full ATPase and transcriptional promoting activities in the absence of effectors (Shingler and Pavel, 1995). DmpR is activated by a wide range of phenolic effector compounds, including substrates of the pathway it controls and some, but not all, structural analogues (Shingler and Moore, 1994; Shingler and Pavel, 1995; O'Neill *et al*., 1999; Shingler, 2004). Effector-binding occurs at a single common site on the A-domain of DmpR (O'Neill *et al*., 1999). However, not all effectors are equal. The magnitude of DmpR-mediated transcription varies depending on the position and nature of substituents on the phenolic ring – differences that have a profound effect on the efficiency with which the bacteria can degrade the corresponding compound (Pavel *et al*., 1994; Sarand *et al*., 2001). Interestingly, while binding affinities determine the concentration at which DmpR responds to the presence of an effector, they do not control the magnitude of the responses (O'Neill *et al*., 1999), suggesting that some phenolics are less effective than others at eliciting conformational changes for downstream events.

Activation of DmpR by its phenolic effectors involves at least two co-ordinated steps: effector-binding and consequent alleviation of repression of the C-domain mediated activities. The B-linker that connects the regulatory A-domain and the catalytic C-domain falls into two functional classes – either serving as flexible linker, or playing a more active role as a structured short coiled-coil, as is the case in DmpR (reviewed in Shingler, 2011). Mutational analysis of the B-linker has shown that this region is critical for both controlling ATPase activity *per se* and for coupling aromatic effector-binding to a transcriptional response (O'Neill *et al*., 2001). As described herein, structural analysis of a truncate of DmpR localized the Y233 residue of the B-linker region to a key location that would predictively hinder ATP hydrolysis. Here, we present evidence that an alanine substitution of Y233 alters both the ATPase activity of DmpR and its ability to respond to aromatic effectors in the context of the full length protein. Based on these findings, we propose a model in which effector-binding relocates Y233 to synchronize signal-reception with multimerisation to allow transcriptional activation of σ^{54}-RNA polymerase.

Results and discussion

Y233 of the B-linker resides in the ATP-binding site of the AAA$^+$ domain

DmpR in its inactive state is predominantly dimeric with a small proportion in a tetrameric conformation, while constitutively active A-domain truncated derivatives and effector-activated DmpR form apparent hexamers in the presence of ATPγS (Wikstrom *et al*., 2001). As illustrated in Fig. 1A, structural analysis of apo C-DmpR – a truncate that encompasses the central AAA$^+$ domain and part of the B-linker – revealed a homo-dimer in a face-to-face orientation with the Y233 residue of the B-linkers located proximal to the P-loops (Walker A motifs) of the two ATP-binding interfaces (Rodrigues *et al*, to be published elsewhere).

To gain insight into potential consequences of the Y233 configuration, C-DmpR was independently superimposed onto structures of nucleotide-bound forms of the AAA$^+$ domains of other bEBPs [ADP-bound to NtrC1 (1NY5_A Lee *et al*., 2003) and ATP-modelled to ZraR (1OJL_E Sallai and Tucker, 2005), with root mean square distances (RMSD) of 0.58 Å and 0.69 Å, respectively; Supporting Information Fig. S1]. As summarized in Fig. 1B, this analysis highlighted a steric clash between the Y233 residue of the B-linker and the adenine moiety of both ATP and its hydrolysis product ADP. Given that ATP-binding is a prerequisite for multimerisation to the active transcription promoting form and ATP-catalysis is intimately involved with activation of σ^{54}-RNAP, these findings suggested that Y233 would likely be important for the functioning of DmpR and may underscore the previously documented role of the B-linker in controlling the ATPase activity of DmpR and co-ordinating activation in response to aromatic effector-binding (O'Neill *et al*., 2001). It is notable that a tyrosine (or a structurally similar phenylalanine) counterpart is conserved in this position within many (> 50%), subclades of effector-responsive bEBPs (Supporting Information Fig. S2).

The Y233A substitution increases sensitivity of DmpR to aromatic effectors in vivo

As a start point to dissect the role of Y233 in DmpR activity, we generated an alanine substituted derivative (Y233A) to minimize the side chain size and thus potential to hinder ATP-hydrolysis. Previous analysis of DmpR has predominantly

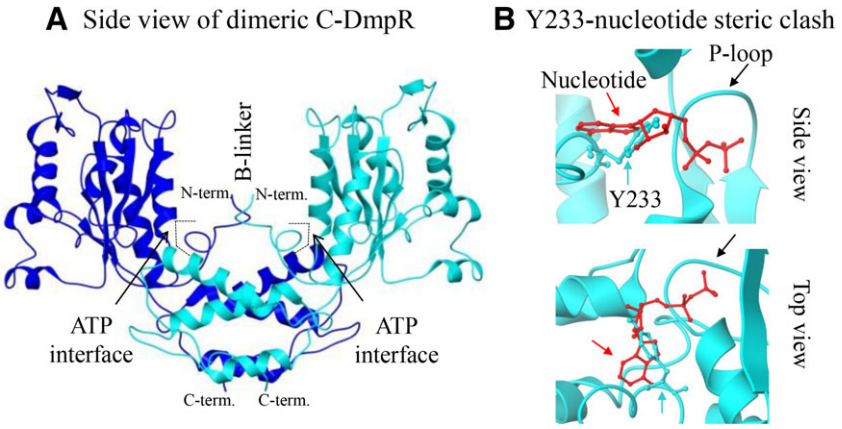

Fig. 1. Y233 of DmpR occludes the ATP-binding site.
A. Ribbon representation of the crystal structure of C-DmpR that encompasses the central AAA$^+$ domain and part of the B-linker of DmpR (amino acids ML_{219} to G_{496}-SHHHHHH). Amino acids D227 to A480 are visible in the electron density of the 1.7 Å resolution structure (Rodrigues *et al*, to be published elsewhere). Two central domains form a homo-dimer in which the N- and C-termini are indicated. The arrows mark the location of the expected ATP-binding interface in each monomer.
B. Close-up view highlighting the steric clash that would arise between the side chain of tyrosine residue Y233 of the B-linker with the adenine base of a nucleotide (stick models) superimposed onto the binding site. ATP-binding is required to initiate dimer reorientation and subsequent multimerisation to the active transcriptional promoting form. The images were obtained by superimposing the crystal structures of the nucleotide bound form of NtrC1 as detailed in Supporting Information Fig. S1.

employed derivatives with a C-terminal Flag- or His-tag, neither of which affect the aromatic effector-activation profile or the level of transcription mediated by DmpR *in vivo* (Shingler and Pavel, 1995; O'Neill *et al*., 1999; 2001). Therefore, we constructed this derivative as gene encoding a C-terminal His-tagged protein on a plasmid under the control of the native Pr promoter of *dmpR.* Activity of this derivative in comparison with the cognate wild-type Pr-*dmpR-His* expression plasmid was monitored using PP980 – a *P. putida* KT2440 strain carrying a Po-*luxAB* transcriptional fusion on its chromosome. Because the σ^{54}-dependent Po promoter is strictly dependent of DmpR for activity, this genetic system provides a direct read-out of active DmpR within the cell.

Comparison of the output from the DmpR-dependent Po promoter revealed major differences in dose responses to both the best effector of DmpR (2-methylphenol) and a poor effector of DmpR (4-methylphenol). Figure 2A and B, show that while expression levels were indistinguishable, the Y233A derivative elicited ~4.5-fold higher output in response to increasing concentrations of 2-methylphenol and up to 12-fold higher output in response to 4-methyphenol. Moreover, A threefold to twelvefold increases in the responses of the Y233A derivative in comparison to the wild-type were also found with a variety of other poor or normally very week effector compounds of DmpR (Fig. 2C). Taken together, these data strongly support the idea that Y233 plays a critical role in mediating responses of DmpR to aromatic effector molecules, presumably through a role in controlling ATP-hydrolysis, and that this is particularly apparent with poor effectors that bind and alleviate A-domain mediated repression ineffectively.

The Y233A substitution enhances ATP-hydrolysis

Having established that the Y233A substitution alters functionality of DmpR *in vivo*, we next turned our attention to the effect of this substitution on ATP-hydrolysis. Within active bEBP hexamers, the catalytic ATP sites are comprised of residues from adjacent back-to-back subunits. Thus, effector activated hexameric DmpR has six catalytic sites. However, noneffector activated (dimeric/tetrameric) DmpR has a substantial basal ATPase activity equivalent to 20% to 30% of the fully activated rate (O'Neill *et al*., 2001; Wikstrom *et al*., 2001), so DmpR can clearly bind and hydrolyse ATP without the ability to promote transcription. This is an innate property of DmpR since a single amino acid substitution (G628S) of the ATP-binding site abolishes both basal and effector-activated ATPase activity as well as its transcriptional promoting capacity (O'Neill *et al*., 1999; Wikstrom *et al*., 2001).

Maximal ATPase activity of DmpR requires ATP in excess of 1.5 mM (Wikstrom *et al*., 2001), therefore, we determined ATP-hydrolysis rates in the presence of 3 mM ATP. Under these conditions, the rate limiting step is predictively ATP-catalysis and/or nucleotide exchange rather than affinity for ATP *per se.* Effector-activated ATPase levels were determined in the presence of a saturating concentration (1 mM) of the most potent effector of DmpR (2-methylphenol). As shown in Fig. 3A, while the Y233A substitution modestly stimulated effector-activated ATPase activity, it dramatically altered basal ATPase activity, by almost doubling ATP turnover rates of this substituted form of the protein (0.78 $\pm$ 0.01 ATP per second per monomer for Y233A as compared to 0.43 $\pm$ 0.02 ATP per second per monomer

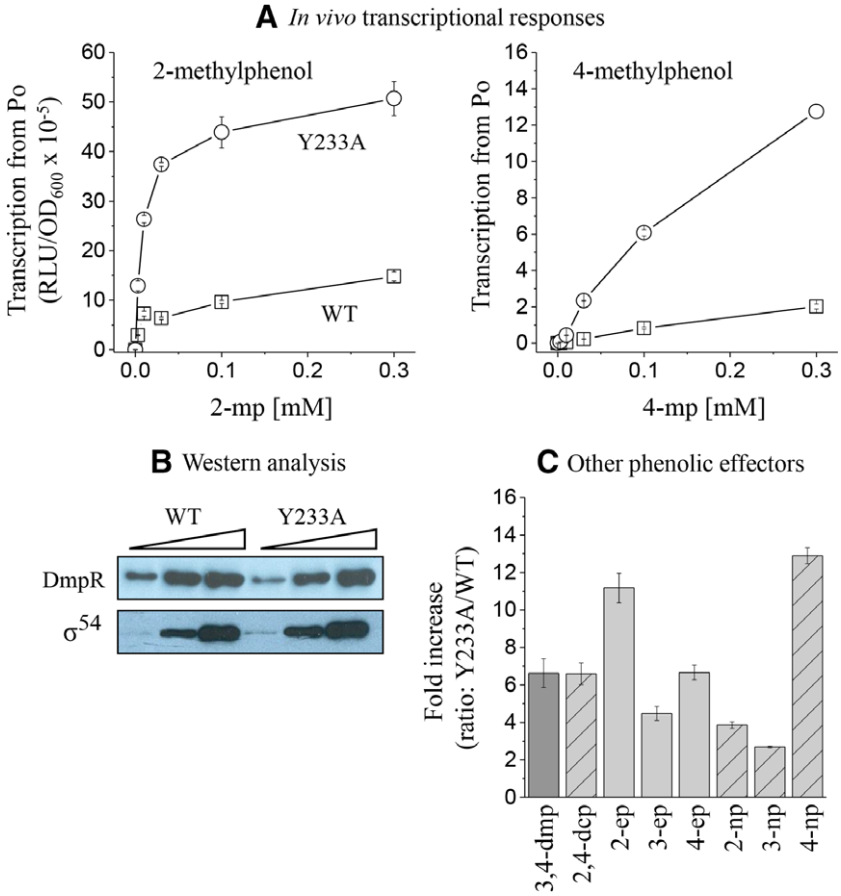

Fig. 2. The Y233A substitution renders DmpR more sensitive to phenolic effectors *in vivo*.
A. Luciferase (Lux) activity assays of the *P. putida* reporter strain carrying Po-*luxAB* on the chromosome (PP980) harbouring plasmids expressing His-tagged DmpR derivatives from the native Pr promoter. Plasmids: of wild-type DmpR (WT, pVI2415, squares) or its Y233A substitution counterpart (Y233A, pVI2416, circles). Strains were cultivated at 30°C in LB in the presence of different concentrations (0, 0.01, 0.03, 0.1, 0.3, 0.1, 0.3 mM) of either 2-methylphenol (2-mp; left) or 4-methylphenol (4-mp; right) for 6 h. Data are the average of triplicate determinations from each of two independent experiments ± *SE*.
B. Western analysis of crude extracts prepared from cells cultured in the presence of 0.1 mM 4-methylphenol as under panel A. Soluble proteins (5, 10 and 20 μg) were separated by 10% SDS-PAGE prior to transfer to membranes and probing with antibodies directed towards DmpR (upper) or RpoN (σ^{54}, lower), which is produced at constant levels over the growth curve and under different growth conditions (Bernardo *et al*., 2009 and references therein) and is used here as a loading control for DmpR levels.
C. Luciferase activity of strains as under panel A in response to 0.1 mM of different phenolic effectors: 3,4-dmp, 3,4-dimethylphenol; 2,4-dcp, 2,4-dichlorophenol; 2-, 3-, 4-ep, -ethylphenol; 2-, 3-, 4-np, -nitrophenol. Graphed values represent the fold increase in DmpR-dependent transcription as a result of the Y233A substitution. Data are the average of triplicate determinations from each of two independent experiments ± *SE*.

for the wild-type). This data supports the notion that Y233 serves a gatekeeping role to constrain the ATPase activity of noneffector activated DmpR – a property that is diminished by the Y233A substitution; and further that this constraint is relieved by effector-activation. That the DmpR B-linker undergoes relocation upon effector-activation is also supported by previous biochemical evidence that the B-linker becomes sensitive to protease cleavage under these conditions (Wikstrom *et al*., 2001).

ATP hydrolysis by DmpR exhibits the unusual property of sensitivity to the ionic strength of the buffer, being inhibited by increasing concentrations of NaCl and KCl (Wikstrom *et al*., 2001). Because effector-activated transition to the active form requires multiple conformational changes of DmpR, it became of interest to determine if the Y233A substitution affects this property. Basal ATP hydrolysis by both DmpR-WT-His and DmpR-Y233A-His are unaffected by 75 mM NaCl (Supporting Information Fig. S3). However, the effector-activated forms of the proteins differed markedly: 50 to 100 mM NaCl reduced ATP hydrolysis by the wild-type protein to approximately 40% of that in the absence of NaCl (squares in Fig. 3B). In contrast, effector-activated ATP hydrolysis by the Y233A substituted derivative was unaffected (or even slightly stimulated) by NaCl (circles in Fig. 3B). Hence, only effector-activated, not basal ATPase activity, is inhibited by increased ionic strength and this property is ameliorated by the Y233A substitution. Taken together, these results establish that the Y233A substitution alters both basal and effector activated ATPase properties of DmpR.

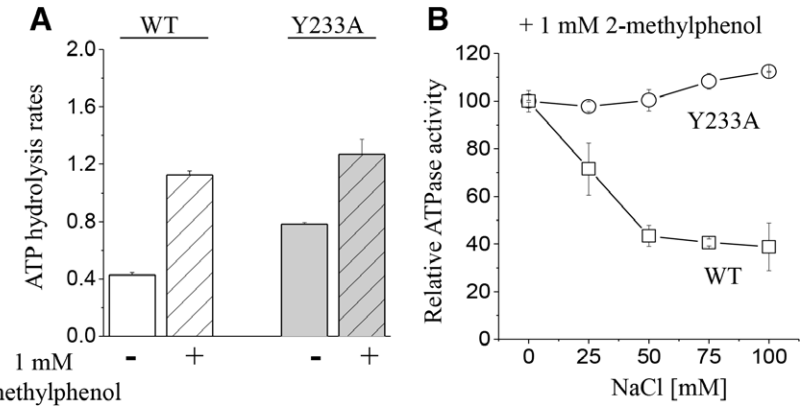

Fig. 3. The Y233A substitution of DmpR alters its ATPase activity.
A. *In vitro* ATP-hydrolysis rates determined using 400 nM DmpR-WT-His (WT) and DmpR-Y233A-His (Y233A) in the absence (open bars) or presence of 1 mM 2-methylphenol (hatched bars), units ATP per second per monomer protein. Note that the Y233A substitution doubles the basal ATPase activity of DmpR. Values are the mean of two independent determinations (quadruplets for basal, triplets for effector activated) ± *SE*.
B. Relative ATP-hydrolysis rates of 400 nM DmpR-WT-His (WT, squares) and DmpR-Y233A-His (Y233A, circles) in the presence of 1 mM 2-methylphenol and the indicated concentrations of NaCl. Note the ion-strength dependent inhibition of ATP-catalyse of the WT, which is not observed with the Y233A derivative. Data for each point is the average ± *SE* of initial ATP-hydrolysis rates from two independent experiments with that in the absence of NaCl set as 100.

The Y233A substitution increases sensitivity to aromatic effectors in vitro

To further investigate the effect of Y233A on DmpR function, we performed single-round *in vitro* transcription assays using native *P. putida* σ^{54}-RNA polymerase. Assays were performed using the same buffer as used for the ATPase assays described above, supplemented with 3 mM ATP. Reactions also included integration host factor (IHF) – a DNA bending protein that increases promoter output by facilitates contact between DmpR bound to its upstream activator sites and promoter bound σ^{54}-RNA polymerase (Sze *et al*., 2001). The transcriptional promoting abilities of untagged native versions of wild-type DmpR and its Y233A counterpart were analysed using a supercoiled plasmid template bearing the σ^{54}-Po promoter with titrations of 2-methyphenol and 4-methyphenol as representatives of potent and poor effectors of DmpR.

As shown in Fig. 4, the same trends as observed in *vivo* were also observed *in vitro*, with the Y233A substituted derivative eliciting higher numbers of transcripts, particularly with the poor effector 4-methylphenol. However, in the presence of high levels of effector, the differential performance of the two proteins was less pronounced as compared to the *in vivo* result, with the Y233A eliciting approximately 1.3- and 2.5-fold higher numbers of transcripts as compared to wild-type in response to near saturating concentrations of 2- and 4-methyphenol, respectively. Muted differences are frequently observed *in vitro* where activities are analysed under conditions that lack competition by other promoters for available components and the macromolecular crowding of intact cells (Kuznetsova *et al*., 2014). Nevertheless, examination of the effector dose–response of the two derivative revealed much greater enhancement of transcription by Y233A with lower concentrations of effector as compared to the wild-type protein (~fourfold and sevenfold for 2-methylphenol and 4-methylphenol, respectively; dashed lines Fig. 4). Given that the A-domain is both necessary and sufficient for binding of the phenolic effector (O'Neill *et al*., 1998), these results suggested to us that Y233A alters the kinetics of effector-stimulated multimerisation to the active form, rather than having an effect on effector-binding *per se.* This interpretation is also supported by the data in Fig. 2.

The Y233A substitution causes accelerated transition to the transcriptional promoting form

Aromatic effector-binding to the A-domain initiates a series of events (ATP-binding triggered reorientation and multimerisation), which lead to the conformation that is competent to interact and activate σ^{54}-RNA polymerase. In standard single-round transcription assays, the regulator is exposed to the effector for a protracted period of time (30 min) prior to participating in initiation of transcription. Because these reactions contain heparin to prevent re-initiation, the number of transcript produced reflects output from the σ^{54}-Po simultaneously occupied by σ^{54}-RNA polymerase and DmpR in its active conformation at equilibrium. Therefore, to be able to monitor effects of the Y233A substitution on the kinetics of effector-driven transition to the active conformation, we modified the assay so that the phenolic effector was added last and samples analysed at different time points after effector addition.

For this series of experiments, subsaturating levels of the phenolic effector was used – 3 μM for 2-methyphenol and 100 μM for the poor effector 4-methylphenol. As anticipated,

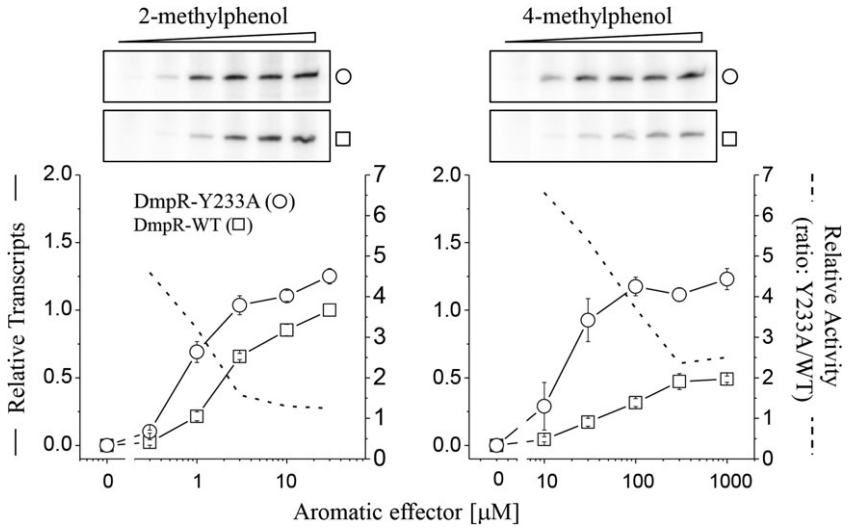

Fig. 4. The Y233A substitution alters DmpR-dependent transcription in response to phenolic effectors.
Single-round *in vitro* transcription assays using 2 nM supercoiled DNA templates (pVI695) harbouring the σ^{54}-dependent Po promoter in the presence of 20 nM *P. putida* σ^{54}-RNAP, 10 nM IHF and 20 nM of the indicated native DmpR derivative. Reactions were performed in the presence of increasing concentrations of 2-methylphenol (left; 0, 0.3, 1, 3, 10, 30 μM) or 4-methyphenol (right; 0, 10, 30, 100, 300, 1000 μM). Insets are images of the 300 nt transcripts from one of two independent experiments used to obtain the graphed average values ± *SE.* Values (arbitrary units) were normalized by setting the number of transcripts of DmpR-WT in the presence of 30 μM 2-methylphenol as 1. Relative responses (dashed lines) were evaluated by dividing those obtained with Y233A by values for the wild-type protein.

the data reveal altered kinetics, which was again particularly apparent with the poor effector (Fig. 5). In the case of the potent effector 2-methyphenol, the kinetic were similar, with Y233A eliciting 3.4-fold higher levels of transcripts than wild-type DmpR at the 10 min time point. However, with 4-methylphenol, maximal levels of transcripts with Y233A were achieved after only 10 min, at which point Y233A elicited 10-fold higher levels than wild-type DmpR. Taken together, the data in Figs 4 and 5 recapitulate the *in vivo* findings (Fig. 2) that Y233 plays a role in constraining the response of DmpR to aromatic effector molecules, and that this is particularly apparent with poor effectors that bind and alleviate A-domain mediated repression inefficiently.

An integrated model for Y233-modulation of coupling between effector activation and the transcriptional promoting form

The data described above show that the Y233A substitution of DmpR modulates both basal and effector-activated ATP turnover rates (Fig. 3 and Supporting Information Fig. S3), demonstrating its key importance for ATP hydrolysis. This substitution also renders the protein hyper-sensitive to activation by its phenolic effectors, leading to increased transcriptional activation both *in vivo* (Fig. 2) and *in vitro* (Fig. 4) – a property that, at least in part, can be traced to altered kinetics of effector-driven transition to the active multimeric form of the protein competent to interact with, and promote transcription by, σ^{54}-RNA polymerase (Fig. 5). The implication of these findings is that the Y233 residue constrains these properties through hindering ATP-catalysis and/or nucleotide exchange.

The simplest model arising from these findings is that binding of the phenolic effector to the A-domain elicits a conformational change that is transduced through the structured B-linker to relocate Y233 from its ATPase gatekeeping location. This, in turn, allows efficient ATP/ADP nucleotide exchange and the subsequent events of ATP-driven reorientation and multimerisation to the active form. Previous biochemical analysis of DmpR has provided evidence that a conformational change upon binding a phenolic effector renders the B-linker sensitive to protease cleavage, and that this change is a prerequisite for ATP-binding triggered multimerisation (Wikstrom *et al*., 2001). More recently, structural determinations of the A-domains of PoxR (Patil *et al*., 2016) and MopR (Ray *et al*., 2016) provide insights into how effector binding might generate movements within the context of the full length protein.

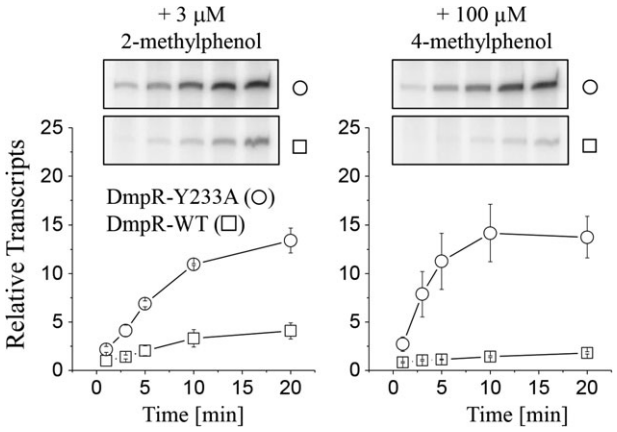

Fig. 5. The Y233A substitution accelerates the kinetics of DmpR-dependent transcription in response to phenolic effectors.
Time-dependent single-round *in vitro* transcription assays using 2 nM supercoiled DNA templates (pVI695) in the presence of *P. putida* 20 nM σ^{54}-RNAP and 10 nM IHF. Reactions were with 20 nM of the indicated native DmpR derivative in the presence of 3 μM 2-methylphenol (left) or 100 μM 4-methylphenol (right). Reactions were incubated for 1, 3, 5 10 or 20 min prior to addition of nucleotides. Insets are images from one of three independent experiments used to obtain the graphed average values ± *SE.* Values (arbitrary units) were normalized by setting the number of transcripts of DmpR-WT in the presence of 3 μM 2-methylphenol after 1 min as 1.

Like DmpR, PoxR and MopR bind multiple phenolic effectors through a single site and possess predicted coiled-coil B-linkers (Fig. 6). The structures of PoxR and MopR are very similar (Fig. 6B), allowing prediction of the structure of the A domain of DmpR by comparative modelling (Fig. 6C). Within these structures, the two B-linkers exit from the outer edges of the dimer, close to the tunnel that leads to the effector-binding pocket. Intriguingly, the A-domains could only be crystalized in the aromatic effector-bound form (Ray *et al*., 2016), indicative of a conformational change upon effector-binding that would likely result in movement of the B-linker within the intact protein. In addition, these studies also highlighted differential movement of one side of the effector-binding pocket when alternative phenolic effectors were bound (Patil *et al*., 2016). The latter finding is interesting, since it suggests that subtle differences in the shape and size of the effector molecule may underscore why some phenolics serve as potent effectors, while others are poor effectors. In this respect, it is intriguing that many of the DmpR A-domain substitutions mutants that alter the effector-sensitivity and/or lead to novel effector responses map to the dimer interface rather than the binding pocket *per se* (Ray *et al*., 2016). Although, speculative, this suggest that the degree of flexibility of the interface of two A-domains may be important in conveying the effector binding signal to the B-linker to ultimately allow efficient ATP-hydrolysis and transcriptional activation by σ^{54}-RNA polymerase.

Concluding remarks

Much attention has been paid to the XylR/DmpR family of ligand activated bEBPs because of their innate ability to bind toxic environmental pollutants and their consequent potential use in biotechnological applications. Enhanced responsiveness of the Y233A substitution to aromatic effectors implies that this residue normally constrains the effector-response of DmpR, and probably also those other DmpR-like proteins that possess a tyrosine or phenylalanine in this position (Supporting Information Fig. S2). In its native context, this is likely an evolutionarily selected desirable property of DmpR that limits transcriptional activation and the production of the metabolically expensive catabolic enzymes until effector concentrations are high enough to give a sufficient metabolic return. On the other hand, anything that constrains responses to an aromatic effector is an undesirable property of sensor-regulators to be employed in biosensor applications and control of artificially engineered pathways (reviewed in Shingler, 2017). Previously, increased sensitivity of DmpR and other similar sensor-regulator of the bEBP family of proteins has primarily deployed substitutions of A-domain residues. This work adds a new approach to the tool box for manipulating effector-responses, and opens up the possibility to combining previous verified A-domain effector-specificity mutations with Y233A to generate ultra-sensitive detectors of aromatic pollutants.

Experimental procedures

Bacterial strains and general procedures

E. coli and *P. putida* KT2440-based strains, alongside plasmids used, are listed in Supporting Information Table S1. Plasmids were constructed by standard molecular techniques as detailed in Supporting Information and were introduced into *E. coli* strains by transformation or *P. putida* strains by electroporation. Selection and maintenance of resident plasmids was insured by the use of either carbenicillin (100 μg/ml for *E. coli*, 1000 μg/ml for *P. putida*) or kanamycin (50 μg/ml) supplements to both liquid and agar solidified Luria-Bertani/Lenox (LB) medium (AppliChem GmbH).

Purified proteins

Native *P. putida* core RNA polymerase and σ^{54} (Johansson *et al*., 2008) native *E. coli* IHF (Sze *et al*., 2001), and ΔA2-DmpR-His (O'Neill *et al*., 2001) were purified as previously described. For the purification of carboxy terminally His tagged full length DmpR derivatives, T7-promoter expression plasmids for DmpR-His (pVI618) and DmpR-Y233A-His (pVI2414) were introduced into BL21(DE3) pLysS. Fresh transformants were grown and induced with IPTG at 19°C prior to preparation and purification from crude extracts on Ni^{2+} and Co^{2+} coupled resin as previously optimized for DmpR-His (O'Neill *et al*., 2001). Peak fractions were pooled, adjusted to 20 mM Tris–HCl pH 7.2, 0.5 M NaCl, 0.25% Triton X Ultra-pure, 1 mM EDTA, 2 mM β-mercaptoethanol with 30% glycerol and stored at –20°C until use.

For purification of native DmpR derivatives, T7-promoter expression plasmids for His-SUMO tagged DmpR (pVI2419) or its Y233A counterpart (pVI2420) were introduced into BL21(DE3). Protein expression and purification was performed by the Protein Expertise Platform (PEP) at Umeå University. In brief, expression was induced using auto-induction media (Studier, 2014) and culturing at 20°C. Peak fractions from Ni^{2+} affinity purification of crude extracts were subject to gel filtration prior to overnight digestion with His tagged SUMO protease. After recovery of post-cleavage native proteins from the flow through from Ni^{2+} coupled resin, proteins were concentrated (Centriprep R, molecular weight cut off 10 000; Merck). The resulting preparations were adjusted to contain 28 mM Tris–HCl pH 8.0, 0.28 M NaCl, 0.14% Triton X Ultra-pure, 0.056% Pluronic F-68, 1 mM EDTA, 0.56 mM β-mercaptoethanol and 50% glycerol and stored at –20°C.

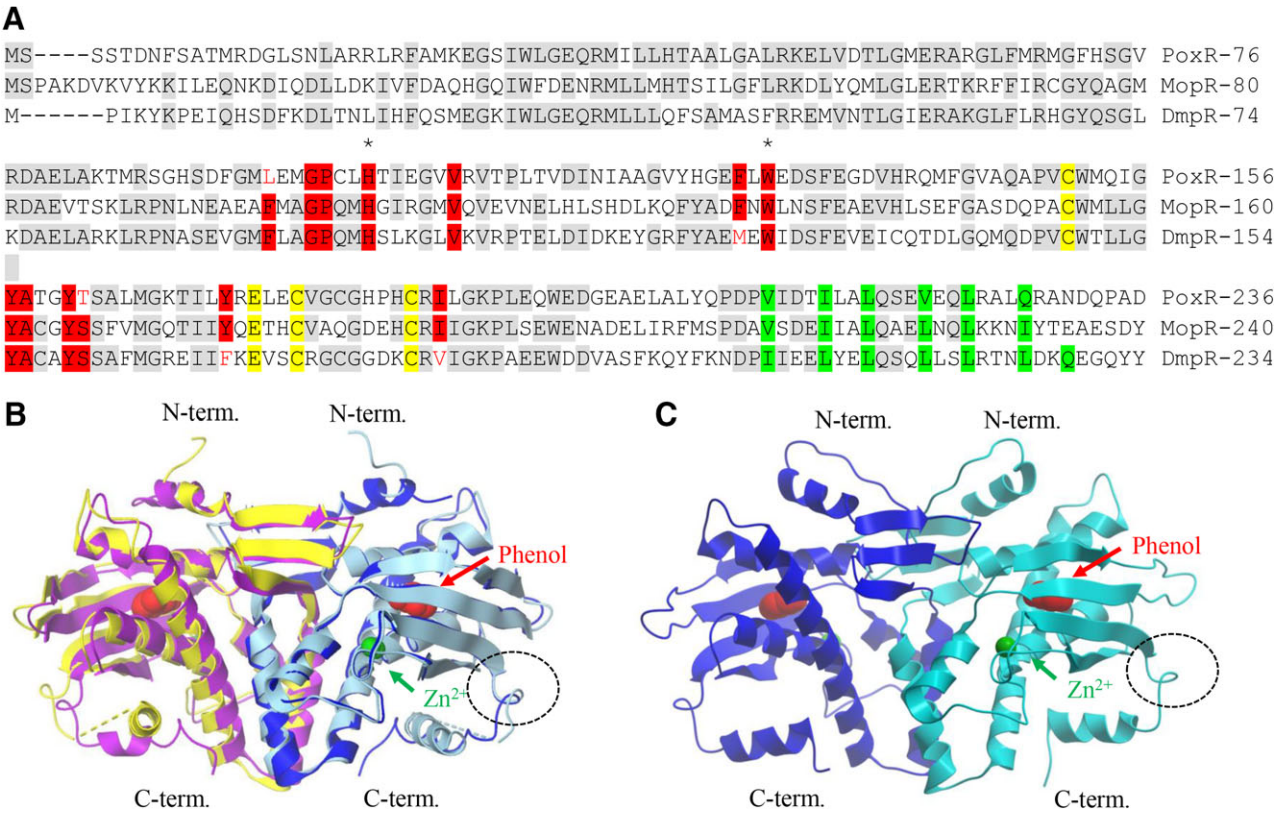

Fig. 6. Comparison of the phenolic effector binding domains of PoxR, MopR and DmpR.
A. Alignment of the A-domain residues of PoxR, MopR and DmpR. Key residues of the phenolic ligand binding pocket are highlighted in red, while residues that co-ordinate the zinc ion are highlighted in yellow. Residues of the B-linker coiled-coil of DmpR (O'Neill *et al*., 2001) and those identified for PoxR and MopR using pcoils (http://toolkit.tuebingen.mpg.de/pcoils; Zimmermann, 2018, p. 494) shown highlighted in green.
B. Superimposition of the dimeric structures of the A-domains of MopR and PoxR. MopR (M1 to K229) is shown as a yellow and light blue ribbon model (PDB code 5KBH), in which amino acids E15 to Q222 are visible in the electron density. PoxR (M1 to I211) is shown as a pink and blue ribbon model, (PDB code 5FRW), in which F8 to D208 are visible in electron density. Structures are shown with a bound phenol (red CPK envelope) and the zinc ion (green sphere), which is important for the structural integrity of the A-domain fold. The dotted circle highlights the exit route of the B-linker from the sensory domain.
C. Comparative model of the DmpR A-domain (residues M1 to E230) built with iTasser (https://zhanglab.ccmb.med.umich.edu/I-TASSER) using the MopR A-domain (PDB code 5KBH) as the template. Only residues M1 to D206 are shown for clarity.

ATPase assay

ATPase assays were performed in a total volume of 30 μl at 30°C essentially as previously described (Wikstrom *et al*., 2001). In brief, assays were performed with DmpR-His or its Y233A derivative in AcB buffer (35 mM Tris-acetate pH 7.9, 5 mM magnesium acetate, 70 mM potassium acetate, 20 mM ammonium acetate, 1 mM DTT). Activities were determined in the absence or presence of 1 mM 2-methylphenol – the most potent effector of DmpR, and in the absence or presence of differing concentrations of NaCl. Reactions were initiated by addition of [γ-^{32}P] ATP (Perkin Elmer) in a dilution of 1:9 to a final concentration of 3 mM. Aliquots (4 μl) of the reactions were taken at 10 min intervals over an hour, adjusted to 0.5% SDS and stored at –20°C until analysed. Samples were boiled for 2 min and 1 μl spotted onto thin layer chromatography polyethyleneimine (PEI) cellulose plates (Merck). Separation of ATP and free Pi by chromatography was performed in 0.75 M KH_2PO_4 buffer (pH 3.5) and quantified using phospho-imaging (Storm 860 imaging system, Molecular Dynamics). Values for the separated free phosphate were calculated as the percentage of the total amount of radioactivity and graphed as a function of time. Initial linear hydrolysis rates were determined for bar and ATP-hydrolysis rate graphs shown.

Luciferase activity assays

Cultures for luciferase activity determinations were grown and assayed at 30°C in LB as described in (Sze *et al*., 1996). Balanced growth was ensured by pre-culturing to the exponential phase prior to a further dilution (to an $OD_{600\ nm}$ of 0.05–0.08) and initiation of the experiment. After 6 h incubation in the absence or presence of an aromatic effector, $OD_{600\ nm}$ and light emission of 100 μl of whole cells was measured upon addition of a 1:2000 dilution of decanal (luciferase substrate) using an Infinite

M200 (Tecan) luminometer. Specific activity is expressed as relative luciferase units per OD_{600} of 1.0.

In vitro *transcription assays*

Single-round *in vitro* assays (20 μl) were performed at 30°C in ATPase acetate buffer (AcB buffer described above) containing 3 mM ATP and 0.275 mg/ml bovine serum albumin as described by (O'Neill *et al*., 2001). Final reaction mixes additionally contained the indicated concentrations of DmpR-derivatives, aromatic effector, NaCl, *P. putida* core RNA polymerase (20 nM), *P. putida* σ^{54} (100 nM), *E. coli* IHF (10 nM) and supercoiled DNA template carrying the DmpR-dependent σ^{54}-Po promoter (2 nM pVI695).

For holoenzyme formation, core RNA polymerase and σ^{54} were pre-incubated for 5 min at 30°C prior to addition of ATP, IHF and DNA template followed by a further incubation for 10 min to allow closed-complex formation. In standard single round assays, DmpR derivatives were premixed with aromatic effectors or a mock solution on ice (10 min) prior to combining with other reaction components and incubation at 30°C for 20 min. Transcription was initiated by the by the addition of NTPs (final concentrations GTP, CTP, ATP 400 nM each; UTP 80 nM, 0.25 μl [α-^{32}P] UTP (Perkin Elmer) in the presence of heparin (0.1 mg/ml) to prevent re-initiation. After 10 min incubation, reactions were terminated by addition of 5 μl of a stop load mix (150 mM EDTA, 1 M NaCl, 14 M urea, 3% glycerol, 0.075% (w/v) xylene cyanol and 0.075% (w/v) bromophenol blue). In time dependent effector-activation experiments, DmpR was directly added to a master mix containing all components except the effector, which was added last. Samples were taken at the indicated times and transcription initiated as described for standard assays. In all cases, transcripts were analysed on a 5% (w/v) polyacrylamide gel containing 7 M Urea and quantified using phospho-imaging.

Western analysis

Cell pellets were washed and re-suspended in ice-cold sonication buffer (20 mM Tris–HCl pH 7.5, 0.2 mM NaCl, 1 mM EDTA) containing protease inhibitors (Complete EDTA-free protease inhibitor tablet; Roche). Cells were disrupted by sonication and samples subsequently clarified by centrifugation. Protein concentrations of the resulting crude extracts were determined with PIERCE BCA protein assay (Thermo Scientific). Soluble protein samples were separated by SDS-PAGE and transferred to PVDF membranes (GE Healthcare) for immune-detection of proteins was performed as described in (Shingler and Pavel, 1995). DmpR derivatives and σ^{54} were detected using polyclonal rabbit antibodies against the amino-terminal 232 residues of DmpR A-domain (Bernardo *et al*., 2006) or the *P. putida* σ^{54} protein (Johansson *et al*., 2008). Antibody-decorated bands were revealed using polyclonal secondary goat anti-rabbit antibodies conjugated with HRP and ECL Plus Western Blotting Reagents (GE Healthcare). Results were recorded using AGFA Curix Ultra UV-G medical X-ray film.

Structure superimposition

All structure superimpositions were carried out using the 'superimpose two proteins' option of the ICM software package (Abagyan *et al*., 1994, Molsoft LLC). Only the backbone atoms of the respective structures were superimposed. ICM was further used to create the images depicting structural models.

Comparative modelling

To create a comparative model of the DmpR A-domain, its amino acid sequence together with the coordinates of the MopR A-domain (PDB code 5KBH), which served as the template, were submitted on-line to the iTasser (Iterative Threading ASSEmbly Refinement) server (https://zhanglab.ccmb.med.umich.edu/I-TASSER).

Acknowledgements

We thank Eleonore Skärfstad for excellent technical assistance and Mikael Lindberg of the Protein Expertise Platform at Umeå University for purified full-length DmpR derivatives. This work was supported by the Swedish Research Council (grant numbers 2011-4791/2016-02047 to VS).

References

Abagyan, R., Totrov, M., and Kuznetsov, D. (1994) Icm - a new nethod for protein modeling and design - applications to docking and structure prediction from the distorted native conformation. *J Comput Chem* **15**: 488–506.

Bernardo, L.M., Johansson, L.U., Skarfstad, E., and Shingler, V. (2009) σ^{54}-promoter discrimination and regulation by ppGpp and DksA. *J Biol Chem* **284**: 828–838.

Bernardo, L.M., Johansson, L.U., Solera, D., Skarfstad, E., and Shingler, V. (2006) The guanosine tetraphosphate (ppGpp) alarmone, DksA and promoter affinity for RNA polymerase in regulation of σ^{54}-dependent transcription. *Mol Microbiol* **60**: 749–764.

Bose, D., Pape, T., Burrows, P.C., Rappas, M., Wigneshweraraj, S.R., Buck, M., and Zhang, X. (2008) Organization of an activator-bound RNA polymerase holoenzyme. *Mol Cell* **32**: 337–346.

Bush, M., and Dixon, R. (2012) The role of bacterial enhancer binding proteins as specialized activators of σ^{54}-dependent transcription. *Microbiol Mol Biol Rev* **76**: 497–529.

Garmendia, J., Devos, D., Valencia, A., and de Lorenzo, V. (2001) *A la carte* transcriptional regulators: unlocking responses of the prokaryotic enhancer-binding protein XylR to non-natural effectors. *Mol Microbiol* **42**: 47–59.

Johansson, L.U., Solera, D., Bernardo, L.M., Moscoso, J.A., and Shingler, V. (2008) σ^{54}-RNA polymerase controls σ^{70}-dependent transcription from a non-overlapping divergent promoter. *Mol Microbiol* **70**: 709–723.

Kuznetsova, I.M., Turoverov, K.K., and Uversky, V.N. (2014) What macromolecular crowding can do to a protein. *Int J Mol Sci* **15**: 23090–23140.

Lee, S.Y., De La Torre, A., Yan, D., Kustu, S., Nixon, B.T., and Wemmer, D.E. (2003) Regulation of the transcriptional activator NtrC1: structural studies of the regulatory and AAA^+ ATPase domains. *Genes Dev* **17**: 2552–2563.

Ng, L.C., O'Neill, E., and Shingler, V. (1996) Genetic evidence for interdomain regulation of the phenol-responsive final σ^{54}-dependent activator DmpR. *J Biol Chem* **271**: 17281–17286.

O'Neill, E., Sze, C.C., and Shingler, V. (1999) Novel effector control through modulation of a preexisting binding site of the aromatic-responsive σ^{54}-dependent regulator DmpR. *J Biol Chem* **274**: 32425–32432.

O'Neill, E., Wikstrom, P., and Shingler, V. (2001) An active role for a structured B-linker in effector control of the σ^{54}-dependent regulator DmpR. *EMBO J* **20**: 819–827.

O'Neill, E., Ng, L.C., Sze, C.C., and Shingler, V. (1998) Aromatic ligand binding and intramolecular signalling of the phenol-responsive σ^{54}-dependent regulator DmpR. *Mol Microbiol* **28**: 131–141.

Patil, V.V., Park, K.H., Lee, S.G., and Woo, E. (2016) Structural analysis of the phenol-responsive sensory domain of the transcription activator PoxR. *Structure* **24**: 624–630.

Pavel, H., Forsman, M., and Shingler, V. (1994) An aromatic effector specificity mutant of the transcriptional regulator DmpR overcomes the growth constraints of *Pseudomonas* sp. strain CF600 on *para*-substituted methylphenols. *J Bacteriol* **176**: 7550–7557.

Rappas, M., Bose, D., and Zhang, X. (2007) Bacterial enhancer-binding proteins: unlocking σ^{54}-dependent gene transcription. *Curr Opin Struct Biol* **17**: 110–116.

Ray, S., Gunzburg, M.J., Wilce, M., Panjikar, S., and Anand, R. (2016) Structural basis of selective aromatic pollutant sensing by the effector binding domain of MopR, an NtrC family transcriptional regulator. *ACS Chem Biol* **11**: 2357–2365.

Sallai, L., and Tucker, P.A. (2005) Crystal structure of the central and C-terminal domain of the σ^{54}-activator ZraR. *J Struct Biol* **151**: 160–170.

Sarand, I., Skarfstad, E., Forsman, M., Romantschuk, M., and Shingler, V. (2001) Role of the DmpR-mediated regulatory circuit in bacterial biodegradation properties in methylphenol-amended soils. *Appl Environ Microbiol* **67**: 162–171.

Schirmer, F., Ehrt, S., and Hillen, W. (1997) Expression, inducer spectrum, domain structure, and function of MopR, the regulator of phenol degradation in *Acinetobacter calcoaceticus* NCIB8250. *J Bacteriol* **179**: 1329–1336.

Shingler, V. (2003) Integrated regulation in response to aromatic compounds: from signal sensing to attractive behaviour. *Environ Microbiol* **5**: 1226–1241.

Shingler, V. (2004)Transcriptional regulation and catabolic strategies of phenol degradation. In *The Pseudomonas Vol II: Virulence and Gene Regulation*, Ramos, J.L. (ed): New York: Kluwer, pp. 451–478.

Shingler, V. (2011) Signal sensory systems that impact σ^{54}-dependent transcription. *FEMS Microbiol Rev* **35**: 425–440.

Shingler, V. (2017)Experimental evolution of novel regulatory activities in response to hydrocarbons and related chemicals . In *Aerobic Utilization of Hydrocarbons, Oils and Lipids Handbook of Hydrocarbon and Lipid Microbiology*, Rojo, F. (ed): Springer, pp. 1–13. doi:10.1007/978-3-319-39782-5_34-1.

Shingler, V., and Moore, T. (1994) Sensing of aromatic compounds by the DmpR transcriptional activator of phenol-catabolizing *Pseudomonas* sp. strain CF600. *J Bacteriol* **176**: 1555–1560.

Shingler, V., and Pavel, H. (1995) Direct regulation of the ATPase activity of the transcriptional activator DmpR by aromatic compounds. *Mol Microbiol* **17**: 505–513.

Shingler, V., Bartilson, M., and Moore, T. (1993) Cloning and nucleotide sequence of the gene encoding the positive regulator (DmpR) of the phenol catabolic pathway encoded by pVI150 and identification of DmpR as a member of the NtrC family of transcriptional activators. *J Bacteriol* **175**: 1596–1604.

Studier, F.W. (2014) Stable expression clones and auto-induction for protein production in *E. coli*. *Methods Mol Biol* **1091**: 17–32.

Sze, C.C., Moore, T., and Shingler, V. (1996) Growth phase-dependent transcription of the σ^{54}-dependent Po promoter controlling the *Pseudomonas*-derived (methyl)phenol *dmp* operon of pVI150. *J Bacteriol* **178**: 3727–3735.

Sze, C.C., Laurie, A.D., and Shingler, V. (2001) *In vivo* and *in vitro* effects of integration host factor at the DmpR-regulated σ^{54}-dependent Po promoter. *J Bacteriol* **183**: 2842–2851.

Tropel, D., and van der Meer, J.R. (2004) Bacterial transcriptional regulators for degradation pathways of aromatic compounds. *Microbiol Mol Biol Rev* **68**: 474–500.

van der Meer, J.R., and Belkin, S. (2010) Where microbiology meets microengineering: design and applications of reporter bacteria. *Nat Rev Microbiol* **8**: 511–522.

Wikstrom, P., O'Neill, E., Ng, L.C., and Shingler, V. (2001) The regulatory N-terminal region of the aromatic-responsive transcriptional activator DmpR constrains nucleotide-triggered multimerisation. *J Mol Biol* **314**: 971–984.

Xue, H., Shi, H., Yu, Z., He, S., Liu, S., Hou, Y., *et al*. (2014) Design, construction, and characterization of a set of biosensors for aromatic compounds. *ACS Synth Biol* **3**: 1011–1014.

Zhang, N., Darbari, V.C., Glyde, R., Zhang, X., and Buck, M. (2016) The bacterial enhancer-dependent RNA polymerase. *Biochem J* **473**: 3741–3753.

Zimmermann, L., Stephens, A., Nam, S.Z., Rau, D., Kubler, J., Lozajic, M., *et al.* (2018) A completely reimplemented MPI bioinformatics toolkit with a new HHpred server at its core. *J Mol Biol* **430**: 2237–2243.

Supporting Information

Additional Supporting Information may be found in the online version of this article at the publisher's web-site:

Appendix S1: Supporting Material